Received 01 July 2020; | Revised ; | Accepted

DOI: xxx/xxxx

RESEARCH ARTICLE

Convective and conductive selection criteria of a stable dendritic growth and their stitching

L.V. Toropova*[1] | D.V. Alexandrov[2] | P.K. Galenko[3]

[1]Laboratory of Mathematical Modeling of Physical and Chemical Processes in Multiphase Media, Department of Theoretical and Mathematical Physics, Ural Federal University, Lenin ave., 51, Ekaterinburg, 620000, Russian Federation

[2]Laboratory of Multi-Scale Mathematical Modeling, Department of Theoretical and Mathematical Physics, Ural Federal University, Lenin ave., 51, Ekaterinburg, 620000, Russian Federation

[3]Physikalisch-Astronomische Fakultät, Friedrich-Schiller-Universität-Jena, 07743 Jena, Germany

Correspondence
*L.V. Toropova. Email: l.v.toropova@urfu.ru

The paper deals with the analysis of stable thermo-solutal dendritic growth in the presence of intense convection. The n-fold symmetry of crystalline anisotropy as well as the two- and three-dimensional growth geometries are considered. The steady-state analytical solutions are found with allowance for the convective-type heat and mass exchange boundary conditions at the dendritic surface. A linear morphological stability analysis determining the marginal wavenumber is carried out. The new stability criterion is derived from the solvability theory and stability analysis. This selection criterion takes place in the regions of small undercooling. To describe a broader undercooling diapason, the obtained selection criterion, which describes the case of intense convection, is stitched together with the previously known selection criterion for the conductive-type boundary conditions. It is demonstrated that the stitched selection criterion well describes a broad diapason of experimental undercoolings.

KEYWORDS:
Dendrites, Dendritic growth, Forced convection, Selection theory, Crystalline anisotropy

1 | INTRODUCTION

Dendritic crystals are frequently encountered growth structures in phase transformations from metastable melts and solutions.[1–10] The growth velocity of dendrites, their shape, and the characteristic size of their tips are determined by the processes of heat and mass transfer at the interphase boundaries, as well as by the anisotropy of surface energy.[11–13] Since the heat and mass transfer completely controls the undercooling (supersaturation) of the liquid created between the surface of the growing dendrite and far from it, the velocity and diameter of the dendritic tips are defined by undercooling of the melt (supersaturation of the solution). Let us especially note that the tip velocity and tip diameter as functions of the undercooling (supersaturation) require determining two equations representing the undercooling (supersaturation) balance condition and the so-called selection criterion.[6,14,15] Such a criterion gives the temperature (solute concentration) distribution in the dendritic tip region, which is in close proximity to the well-known parabolic (paraboloidal) distributions found for the first time by Ivantsov and Horvey-Cahn.[16–19] It is significant to highlight that the selection criterion was derived in a series of previous papers in the case of conductive heat and mass transfer mechanism at the dendritic surface[20–28] accounting for the effects of forced flows, binary systems, attachment kinetics of atoms, and rapid solidification.

An important point is that the convective type of heat and mass transfer boundary conditions at the growing dendritic surfaces drastically changes the crystallization scenario in the presence of intense convection in liquid. This, for example, occurs in the presence of oceanic (turbulent) flows under the growing dendritic ice cover.[29,30] If this is really the case, we need to determine

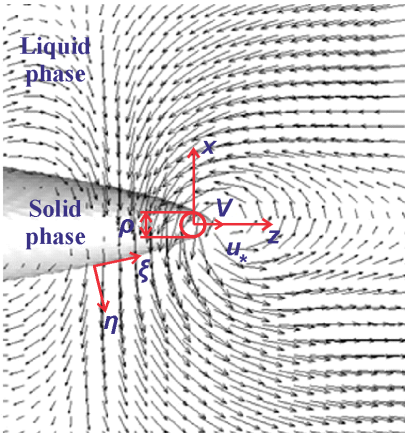

FIGURE 1 A scheme of growing dendritic crystal in an intense convective (turbulent) flow.

the selection criterion for the convective boundary conditions by analogy with the frequently met crystallization scenario with conductive boundary conditions. To do this, we use the solvability theory developed by Pelcé and Bensimon.[31] To find the marginal mode of the wave-number and substitute it into the solvability condition,[31] we develop the morphological stability theory for convective boundary conditions, which enables to derive this wave-number. Since the convective criterion works in the vicinity of dendritic tip region, we then sew together the convective and conductive selection criteria to find a single one working in a wide diapason of the melt undercooling.

2 | THE CRYSTAL GROWTH MODEL AND ITS STATIONARY SOLUTION

Let us describe the model of thermo-solutal dendritic growth in the case of intense convection in liquid. The convective heat and mass transport equations in the solid and liquid phases take the form

$$\frac{\partial T_l}{\partial t} + (\mathbf{w}\cdot\boldsymbol{\nabla})\, T_l = D_T \nabla^2 T_l, \;\; \frac{\partial T_s}{\partial t} = D_T \nabla^2 T_s, \tag{1}$$

$$\frac{\partial C_l}{\partial t} + (\mathbf{w}\cdot\boldsymbol{\nabla})\, C_l = D_C \nabla^2 C_l, \tag{2}$$

where $\mathbf{w}$ is the fluid velocity, T_l and T_s are the temperatures in the liquid and solid phases, D_T is the thermal diffusivity, D_C is the diffusion coefficient, C_l is the solute concentration in liquid, t is the time variable, and subscripts s and l designate the solid and liquid phases.

If the fluid field near the crystal surface is substantial, the dendrite growth depends on convective heat and mass (or turbulent) fluxes in liquid (figure 1 illustrates an isolated dendrite growing in a convective flow). Taking this into account let us write out the boundary conditions on the crystal surface as[29,30,32–34]

$$\frac{T_Q}{D_T}\mathbf{v}\cdot\mathbf{n} = \nabla T_s \cdot \mathbf{n} + \frac{\alpha_h \rho_l c_l u_*}{k_s}\left(T_i - T_\infty\right), \tag{3}$$

$$\left(1-k_0\right) C_i \mathbf{v}\cdot\mathbf{n} = \alpha_m u_* \left(C_i - C_{l\infty}\right). \tag{4}$$

Here $\mathbf{v}\cdot\mathbf{n}$ is the normal growth velocity, T_Q represents the hypercooling, α_h and α_m are the convective (turbulent) coefficients for heat and mass, k_s is the coefficient of thermal conductivity in the solid phase, c_l is the heat capacity of the liquid phase, T_i and C_i are the temperature and concentration at the interface of the dendrite, T_∞ and $C_{l\infty}$ are the temperature and solute concentration far from the denrite interface, k_0 is the segregation coefficient, and u_* is the friction velocity. This velocity is defined by the shear stress τ_s and the liquid phase density ρ_l as $u_* = \sqrt{\tau_s/\rho_l}$.[35] Let us especially note that $\alpha_h/\alpha_m = \left(D_T/D_C\right)^{\bar{n}}$, where $2/3 < \bar{n} < 4/5$.[36–38]

The Gibbs-Thomson equation at the solid-liquid boundary reads as

$$T_i = T_0 - mC_i - T_Q d(\theta)\mathcal{K} - \tilde{\beta}(\theta)\mathbf{v}\cdot\mathbf{n}, \tag{5}$$

where T_0 is the phase transition temperature at the planar interface of a single-component melt, and m is the liquidus slope.

The solid-liquid interface curvature is given by

$$\mathcal{K} = \begin{cases} 1/R, & \text{two} - \text{dimensional space} \quad \text{(2D case)}, \\ (R_1 + R_2)/(R_1 R_2), & \text{three} - \text{dimensional space} \quad \text{(3D case)}, \end{cases} \tag{6}$$

where R is the dendrite tip radius in 2D, R_1 and R_2 are the main radii of curvature for dendritic tip in 3D.

The capillary length $d(\theta)$ and the function of anisotropic kinetics $\tilde{\beta}(\theta)$ are described by

$$d(\theta) = d_0 \left\{1 - \alpha_d \cos\left[n\left(\theta - \theta_d\right)\right]\right\}, \tag{7}$$

$$\tilde{\beta}(\theta) = \beta_0 T_Q \left\{1 - \alpha_\beta \cos\left[n\left(\theta - \theta_\beta\right)\right]\right\}, \tag{8}$$

where d_0 and β_0 are the capillary and kinetic constants, $\alpha_d \ll 1$ is the stiffness which depends on ε_c (small anisotropy parameter of surface energy), $\alpha_\beta \ll 1$ is the kinetic anisotropy parameter, θ_d and θ_β are the angles between the growth directions and minimal functions $d(\theta)$ and $\tilde{\beta}(\theta)$, n is the order of crystalline symmetry. Note that equations (7) and (8) were averaged over the polar angle.[39]

Further the equations (1) and (2) can be integrated in the parabolic/paraboloidal coordinates ξ and η (2D case) or ξ, η and φ (3D case), which are connected with the Cartesian coordinates x, y and z as

$$\begin{aligned} x = \rho\sqrt{\xi\eta}, \quad z = \frac{\rho(\eta - \xi)}{2} \quad (2D), \\ x = \rho\sqrt{\xi\eta}\cos\varphi, \quad y = \rho\sqrt{\xi\eta}\sin\varphi, \quad z = \frac{\rho(\eta - \xi)}{2} \quad (3D), \end{aligned} \tag{9}$$

where ρ represents the dendritic tip diameter, φ is the polar angle lying in the plane that is perpendicular to the incoming flow, and $\eta = 1$ determines the solid/liquid surface of a dendrite.

Taking the boundary conditions (3) and (4) into consideration, one can obtain the temperature and solute concentration in the liquid phase dependent only on the distance η from a dendrite

$$T_l(\eta) = T_i + (T_\infty - T_i)\frac{I_T(\eta)}{I_T(\infty)}, \quad C_l(\eta) = C_i + (C_{l\infty} - C_i)\frac{I_C(\eta)}{I_C(\infty)}, \tag{10}$$

$$\begin{aligned} I_T(\eta) = \int_1^\eta \frac{\exp\left(-P_g\eta'\right)}{\eta'^{(j-1)/2}}d\eta', \quad I_C(\eta) = \int_1^\eta \frac{\exp\left(-P_C\eta'\right)}{\eta'^{(j-1)/2}}d\eta', \\ T_i = T_\infty + \frac{T_Q V k_s}{\alpha_h \rho_l c_l u_* D_T}, \quad C_i = \frac{\alpha_m u_* C_{l\infty}}{\alpha_m u_* - (1 - k_0)V} \end{aligned} \tag{11}$$

with $j = 2$ (2D case) and $j = 3$ (3D case). Here $P_g = \rho V/(2D_T)$ and $P_C = \rho V/(2D_C)$ stand for the growth Péclet numbers determined for the temperature and concentration fields (V is the steady-state velocity of dendritic growth).

Next section is devoted to the behavior of morphological perturbations concerning these quasistationary solutions.

3 | LINEAR STABILITY ANALYSIS AND SOLVABILITY INTEGRAL

Linear stability analysis determines a response of dendritic surface near the tip region to small perturbations in the case of convective heat and mass transfer. In this instance, the main idea of the analysis is to find the marginal mode (between instability and stability) from the critical value of the wave number $k = k_m$ by analogy with the previously developed theory.[4,6,21]

Let us introduce the special coordinate system (x_c, y_c), which is connected with the crystal surface, and x_c and y_c designate the tangent and normal axes to the crystal surface. Also, note that the origin of this frame of reference is at the dendritic surface and θ represents the angle between the surface normal and growth axis. So, the small perturbations of temperature and solute

concentration fields following from (1) and (2) satisfy the equations

$$\begin{aligned}\frac{\partial T'_{l,s}}{\partial t}+\bar{u}\frac{\partial T'_{l,s}}{\partial x_c}+\bar{v}\frac{\partial T'_{l,s}}{\partial y_c}+v'\frac{d\bar{T}_{l,s}}{dy_c}=D_T\nabla^2 T'_{l,s},\\ \frac{\partial C'_l}{\partial t}+\bar{u}\frac{\partial C'_l}{\partial x_c}+\bar{v}\frac{\partial C'_l}{\partial y_c}+v'\frac{d\bar{C}_l}{dy_c}=D_C\nabla^2 C'_l,\end{aligned} \tag{12}$$

where $\bar{u}=-V\sin\theta$ and $\bar{v}=-V\cos\theta$.

The morphological perturbations for the temperature fields T'_l and T'_s in the liquid and solid phases, the solute concentration C'_l and the crystal surface ξ' can be written out as

$$\begin{aligned}T'_l(x_c,y_c,t)=(T_{l0}+T_{l1}y_c+T_{l2}y_c^2)E(x_c,y_c,t),\quad T'_s(x_c,y_c,t)=(T_{s0}+T_{s1}y_c+T_{s2}y_c^2)E(x_c,y_c,t),\\ C'_l(x_c,y_c,t)=(C_{l0}+C_{l1}y_c+C_{l2}y_c^2)E(x_c,y_c,t),\quad \xi'(x_c,y_c,t)=CE(x_c,y_c,t),\end{aligned} \tag{13}$$

where $E(x_c,y_c,t)=\exp\left(\omega t+ikx_c-\epsilon k y_c\right)$, $\partial\xi'/\partial t=-v'$, $T_{l\iota}$, $T_{s\iota}$, C_ι and C stand for the corresponding amplitudes, k and ω are the wavenumber and frequency of perturbations ($\iota=0,1,2$); i is the imaginary unit, and $\epsilon=1$ or -1 (its sign coincides with the sign of real part of k as disturbances cannot be diverging).

Combining expressions (12) and (13), we arrive at the following amplitudes

$$\begin{aligned}T_{l,s2}=\frac{\omega C}{4D_T}\frac{d\bar{T}_{l,s}}{dy_c},\quad T_{l,s1}=\frac{3\omega C}{4\epsilon k D_T}\frac{d\bar{T}_{l,s}}{dy_c}-\frac{[\omega+Vk(\epsilon\cos\theta-i\sin\theta)]\,T_{l,s0}}{2\epsilon k D_T},\\ C_2=\frac{\omega C}{4D_C}\frac{d\bar{C}_l}{dy_c},\quad C_1=\frac{3\omega C}{4\epsilon k D_C}\frac{d\bar{C}_l}{dy_c}-\frac{[\omega+Vk(\epsilon\cos\theta-i\sin\theta)]\,C_0}{2\epsilon k D_C}.\end{aligned} \tag{14}$$

Note that the derivatives $d\bar{T}_l/dy_c=h_1$ and $d\bar{C}_l/dy_c=h_2$ at the crystal interface are defined by expressions (10) and (11) and take the form

$$h_1=-\frac{2T_Q V k_s\exp(-P_g)}{\rho\alpha_h\rho_l c_l u_* D_T I_T(\infty)},\quad h_2=-\frac{2(1-k_0)VC_{l\infty}\exp(-P_C)}{\rho\left[\alpha_m u_*-(1-k_0)V\right]I_C(\infty)}. \tag{15}$$

Now expanding expressions (3)-(5) in series at the crystal surface $y_c=0$, we arrive at four equations for the morhological perturbations

$$\begin{aligned}T'_l=-(h_1+mh_2)\xi'-mC'_l-dT_Q\frac{\partial^2\xi'}{\partial y_c^2}+\tilde{\beta}\frac{\partial\xi'}{\partial t},\quad T'_s=mh_2\xi'+mC'_l+dT_Q\frac{\partial^2\xi'}{\partial y_c^2}-\tilde{\beta}\frac{\partial\xi'}{\partial t},\\ \frac{T_Q}{D_T}\frac{\partial\xi'}{\partial t}=\frac{\partial T'_s}{\partial y_c}-2bh_1\xi'-2bT'_l,\quad \frac{1-k_0}{\alpha_m u_*}\left(V\cos\theta C'_l+V\cos\theta h_2\xi'+C_i\frac{\partial\xi'}{\partial t}\right)+C'_l+h_2\xi'=0,\end{aligned} \tag{16}$$

where $b=\alpha_h\rho_l c_l u_*/(2k_s)$.

Now combining the morphological perturbations (13) and the boundary conditions (16) at $y_c=0$, we come to the equations for T_{l0}, T_{s0}, C_{l0} and C. Eliminating these amplitudes from this set of four equations, we come to the dispersion law $\omega(k)$. Let us now take into account that the real perturbation evolves with a shift $-iVk\sin\theta$ in the dispersion law $\omega(k)-iVk\sin\theta$ if the frame of reference is moving in the z-direction with a constant velocity V.[21,22] Keeping this in mind, chosing $\epsilon=-1$ and replacing i by $-i$,[21] we arrive at the equation for marginal mode $k=k_m$ of the wavenumber at the neutral stability surface (where $\omega=0$)

$${k_m}^2+\left(2b-\frac{i\beta V\sin\theta}{d}-\frac{iB\sin\theta}{dA}\right)k_m-\frac{2bi\beta V\sin\theta}{d}-\frac{iV\sin\theta}{D_T d}-\frac{2biB\sin\theta}{dA}=0, \tag{17}$$

where

$$A=1+\frac{(1-k_0)V\cos\theta}{\alpha_m u_*},\quad B=\frac{(1-k_0)mC_iV}{\alpha_m u_* T_Q},\quad \beta(\theta)=\frac{\tilde{\beta}(\theta)}{T_Q}.$$

To obtainn the selection criterion (expression for V and ρ), the marginal wavenumber k_m found from equation (17) should be substituted into the following solvability condition derived by Pelcé and Bensimon[31]

$$\int_{-\infty}^{\infty}G\left[X_0(l)\right]Y_m(l)dl=0,\ Y_m(l)=\exp\left[i\int_0^l k_m(l_1)dl_1\right], \tag{18}$$

where G designates the curvature operator, and $X_0(l)$ is a continuum of solutions from which the dependence $k_m(l)$ can be deduced.

4 | SELECTION CRITERION IN THE CASE OF N-FOLD SYMMETRY OF DENDRITIC GROWTH

In this section, we analyze the solvability integral (18) with allowance for the wavenumber k_m given by expression (17). First, considering various dendritic growth modes with convective heat and mass transfer, we derive the corresponding criterion for selecting a stable growth scenario. Then this criterion will be sewed together with the previously derived selection criterion for the conductive conditions of heat and mass transfer on the dendrite surface.

4.1 | Selection criterion for purely thermal dendritic growth with convective boundary conditions

Equation (17) in the absence of solute concentration ($C_{l\infty} = 0$ and $C_i = 0$) gives

$$k = -b\sqrt{1 + \frac{iqV\sin\theta}{bd}} - b + \frac{i\beta V\sin\theta}{2d}, \tag{19}$$

where $q = \beta_0 + 1/(bD_T)$, $\alpha_\beta \ll 1$ and $V \lesssim 10$ m/s.

Now combining expressions (18) and (19) in the case of small anisotropies $\alpha_d \ll 1$, $\alpha_\beta \ll 1$ and considering $\theta_d = 0$,[1] one can get

$$\int\limits_{-\infty}^{\infty} d\phi G\left[X_0(\eta(\phi))\right]\exp\left\{\int\limits_{1/\sqrt{2\alpha_d}}^{\phi}\left[\sqrt{\frac{2^{7/4}\rho^2 bqV\alpha_d^{5/n}A_n^{5/n}\left(\phi'^{\frac{n+1}{2}} - \tilde{\tau}\phi'(\phi'^{n/2}-1)\right)}{d_0\left(1-\phi'^{n/2}\right)}}\right.\right.$$
$$\left.\left. + \frac{\rho A_n{}^{2/n}}{\sqrt{2}d_0\alpha_d^{1-2/n}}\left(2^{7/4}\alpha_d^{1+1/n}A_n^{1/n}bd_0\sqrt{\phi'} + \beta_0 V\alpha_\beta\right)\right]d\phi'\right\} = 0, \tag{20}$$

where

$$\tilde{\tau} = \tau A_n^{1/n}\alpha_d^{\frac{(n-1)(n-4)}{4n}}, \quad \tau = \frac{2^{3/4}\alpha_d^{\frac{5-n}{4}}bd_0}{qV}, \quad A_n = 2^{-3n/4}\sum_{k=0}^{n}\binom{n}{k}i^{n-k}\cos\frac{(n-k)\pi}{2}.$$

Here the following substitutions are taken into account[6,21]

$$I_1 = -\frac{\rho}{2}\left[\frac{\tan\theta}{\cos\theta} + \ln\left(\frac{1}{\cos\theta} + \tan\theta\right)\right],\ \eta(\phi) = \tan\theta = i\left(1 - \sqrt{2\alpha_d}\phi\right),\ \phi = \frac{A_n^{2/n}\phi'}{\alpha_d^{(n-4)/(2n)}},\ \alpha_d \approx \alpha_\beta \ll 1.$$

The integral equation (20) has two main contributions. The first one is the contribution from the stationary phase points, which reads as

$$\cos\left[\bar{A}_2\sqrt{\frac{\rho^2 bqV\alpha_d^{5/n}A_n^{5/n}}{d_0}}\left(1 + \bar{B}_2\tilde{\tau}^{\frac{n+5}{2(n-1)}}\right) + \frac{2a_1(1-\tilde{\tau}^{\frac{3}{n-1}})}{3} + a_2\left(1 - \tilde{\tau}^{\frac{2}{n-1}}\right)\right]. \tag{21}$$

The second one is the contribution from the loop (between the distance $\sim \tilde{\tau}^{2/(n-1)}$) at the intersection of the sharp descent trajectory and the real axis and $\phi' \sim 1$. In this case, an oscillating factor of the exponentially small value of the integral can be written out as

$$\cos\left[\bar{A}_1\sqrt{\frac{\rho^2 bqV\alpha_d^{5/n}A_n^{5/n}}{d_0}}\left(1 + \bar{B}_1\tilde{\tau}^{\frac{n+5}{2(n-1)}}\right) + \frac{2a_1}{3}\tilde{\tau}^{\frac{3}{n-1}} + a_2\tilde{\tau}^{\frac{2}{n-1}}\right], \tag{22}$$

$$a_1 = 2^{5/4}A_n^{3/n}\alpha_d^{3/n}\rho b, \quad a_2 = \frac{\alpha_\beta A_n^{2/n}\rho\beta_0 V}{\sqrt{2}d_0\alpha_d^{\frac{n-2}{n}}}.$$

Here $\bar{A}_1$, $\bar{A}_2$, $\bar{B}_1$ and $\bar{B}_2$ are constans.

Setting equal to zero the sum of contributions (21) and (22), we obtain the solvability (selection) criterion of dendrite growth in a pure substance in the case of convective heat transfer in the liquid phase

$$\sigma^* = \frac{2d_0D_T}{\rho^2V} = \frac{\sigma_0\alpha_d^{5/n}A_n^{5/n}\left(1+bD_T\beta_0\right)\left(1+\mu\tilde{\tau}^{\frac{n+5}{2(n-1)}}\right)^2}{\left[1+\nu_1\left(\alpha_d^{3/n}A_n^{3/n}\rho b+\frac{3\alpha_d^{1/4}A_n^{2/n}\rho\beta_0V}{2^{5/4}d_0}\right)\right]^2}, \tag{23}$$

where $\nu_1^2 = 2^{9/2}25\sigma_0/27$, σ_0 and μ are constants determined from the experimental tests[40] or phase field simulation methods.[41,42]

4.2 | Selection criterion for thermo-solutal dendrite growth with convective boundary conditions

Let us now introduce $\beta_1 = \beta_0 + mC_i(1-k_0)/(T_Q\alpha_m u_*)$. In the limit of very dilute systems $\beta_1 \ll \sqrt{d_0/(VD_T)}$ or $\beta_1 \ll bd_0/V$ and $A \sim 1$, the wave number k_m can be found from expression (19), where β_0 is replaced by β_1, and the selection criterion becomes

$$\sigma^* = \frac{\sigma_0\alpha_d^{5/n}A_n^{5/n}\left(1+bD_T\beta_1\right)\left(1+\mu\tilde{\tau}_1^{\frac{n+5}{2(n-1)}}\right)^2}{\left[1+\nu_1\left(\alpha_d^{3/n}A_n^{3/n}\rho b+\frac{3\rho\alpha_d^{1/4}A_n^{2/n}\beta_1V}{2^{5/4}d_0}\right)\right]^2}, \quad \tilde{\tau}_1 = \frac{\alpha_d^{1/n}A_n^{1/n}\rho b^2d_0}{2^{1/4}P_g(1+bD_T\beta_1)}. \tag{24}$$

Considering now the case $\beta_1 \gg \sqrt{d_0/(VD_T)}$, we obtain from (17)

$$k = \frac{i\beta_1V\sin\theta}{d}. \tag{25}$$

Further, combining expressions (18) and (25), we arrive at

$$\int\limits_{-\infty}^{\infty} d\phi G\left[X_0(\eta(\phi))\right]\exp\left(\frac{\sqrt{2}\rho V\beta_1\alpha_d^{2/n}A_n^{2/n}}{d_0}\int\limits_{1/\sqrt{2\alpha_d}}^{\phi}\frac{\phi'^{n/2}d\phi'}{\phi'^{n/2}-1}\right) = 0, \tag{26}$$

where the contribution from the loop is written in the form of

$$\cos\left(\frac{\bar{A}_3\rho V\beta_1\alpha_d^{2/n}A_n^{2/n}}{d_0}\right) = 0 \tag{27}$$

and $\bar{A}_3$ is a constant.

Now equating (27) to zero, we come to the selection criterion

$$\sigma^* = \frac{2d_0D_T}{\rho^2V} = \frac{2\sigma_0D_T\beta_1\alpha_d^{2/n}A_n^{2/n}}{\rho}, \tag{28}$$

where σ_0 represents a constant, which can be found again by the phase field modeling or experimentally (here the limit of applicability is $\beta_1 \gg \sqrt{d_0/(VD_T)}$).

The generalized selection criterion for both limiting cases in β_1 can be written as

$$\sigma^*(\rho,V) = \sigma^*_{conv}(\rho,V) = \frac{2d_0D_T}{\rho^2V} = \frac{\sigma_0\alpha_d^{5/n}A_n^{5/n}\left(1+bD_T\beta_1\right)\left(1+\mu\tilde{\tau}_1^{\frac{n+5}{2(n-1)}}\right)^2}{\left[1+\nu_1\left(\alpha_d^{3/n}A_n^{3/n}\rho b+\frac{3\alpha_d^{1/4}A_n^{2/n}P_g\beta_1D_T}{2^{1/4}d_0}\right)\right]^2}+\frac{2\sigma_0\alpha_d^{2/n}A_n^{2/n}D_T\beta_1}{\rho}. \tag{29}$$

Consequently, the selection criterion (29) defines a combination between the dendrite growth velocity V and its tip diameter ρ in the case of convective heat and mass transfer in liquid and n-fold symmetry order of crystalline anisotropy. An important point is that the selection criterion (29) transforms to the previously developed theory with the four-fold order of the crystalline symmetry ($n = 4$).[6]

4.3 | Selection criterion for the thermo-solutal dendritic growth with conductive boundary conditions

Following the paper by Alexandrov et al.,[6] let us write down the selection criterion that describes the stable crystal growth with conductive heat and mass transfer boundary conditions at the dendritic surface

$$\sigma^*(\rho,V)=\sigma^*_{cond}(\rho,V)=\frac{2d_0D_T}{\rho^2V}=\frac{\sigma_0\alpha_d^{7/n}A_n^{7/n}}{1+\tilde{b}\bar{\tau}_n^{\upsilon_n}}\left\{\frac{1}{\left[1+a_{1n}\alpha_d^{2/n}A_n^{2/n}P_g\left(1+\delta_0D_T\beta_0/d_0\right)\right]^2}+\frac{2mC_i(1-k_0)D_T}{\left[1+a_{2n}\alpha_d^{2/n}A_n^{2/n}P_C\left(1+\delta_0D_C\beta_0/d_{0\mathrm{CD}}\right)\right]^2T_QD_C}\right\},\tag{30}$$

where

$$\bar{\tau}_n=\alpha_d^{-3/n}A_n^{-3/n}\left(\frac{aUd_0}{4\rho VP}+\frac{aUd_0D_T}{2\rho VPD_C}\right),\ P=1+\frac{2mC_i(1-k_0)D_T}{T_QD_C},\ \upsilon_n=\frac{n+7}{2(n+3)},$$

$$a_{1n}=\left(\frac{8\sigma_0}{7}\right)^{1/2}\left(\frac{3}{56}\right)^{3/8}A_n^{3/(2n)}\alpha_d^{(12-3n)/(8n)},\ a_{2n}=\sqrt{2}a_{1n},\ d_{0\mathrm{CD}}=\frac{T_Qd_0}{2mC_i(1-k_0)},\ \delta_0=20\sqrt{\frac{7}{24}}\left(\frac{56}{3}\right)^{3/8}.$$

Here k_0 is the equilibrium segregation coefficient, $\tilde{b}$ is a hydrodynamic selection constant, and parameters C_i and a should be substituted from expressions (2.15) and (3.3) (for details, see our previous theory[6]).

This criterion describes a stable mode of dendritic growth in a forced hydrodynamic flow with velocity U directed in the opposite direction to the crystal growth axis.[6] Let us also especially underline that expression (30) can be generalized considering the case of rapid crystallization.[25,26]

4.4 | Stitching together the "convective" and "conductive" selection criteria

It is significant to note that the selection criterion (29) describes the case of convective heat and mass transfer boundary conditions on the dendritic surface. It means that this criterion works when such a transfer mechanism predominates. This, in turn, occurs at sufficiently intense convection (e.g., in the case of turbulent flows in the ocean) and small undercoolings ΔT. From the other hand, the selection criterion (30) describes the classical conductive heat and mass transfer mechanism, which works in a broad range of undercoolings when the convective type of heat and mass transfer can be neglected in comparison with the conductive one. Therefore, to obtain a generalized criterion, we need stitching together the "convective" and "conductive" selection criteria (29) and (30).

Using a simple power form for the stitching functions $b_{cond}(\Delta T)$ and $b_{conv}(\Delta T)$, we arrive at a generalized selection critrerion, which reads as

$$\sigma^*_{gen}=\frac{2d_0D_T}{\rho^2V}=\frac{\sigma^*_{conv}b_{conv}(\Delta T)+\sigma^*_{cond}b_{cond}(\Delta T)}{b_{conv}(\Delta T)+b_{cond}(\Delta T)}.\tag{31}$$

Here the subscript gen designates a generalized selection criterion, whereas subscripts $conv$ and $cond$ mean the convective and conductive contributions. As this takes place, the stitching functions are introduced as follows

$$b_{conv}(\Delta T)=\epsilon_{conv}\left(\frac{T_Q}{\Delta T}\right)^{j_{conv}},\quad b_{cond}(\Delta T)=\epsilon_{cond}\left(\frac{\Delta T}{T_0}\right)^{j_{cond}},\tag{32}$$

where $\epsilon_{conv}=(T_Q/T_0)^{i_{conv}}\ll 1$, $\epsilon_{cond}=(T_Q/T_0)^{i_{cond}}\ll 1$, and $i_{conv}>1$, $i_{cond}>1$, $j_{cond}>1$ and $j_{conv}>1$ are the fitting constants. These parameters should be chosen in such a way as to achieve the best possible stitching of functions $\sigma^*_{conv}(\rho,V,\Delta T)$ and $\sigma^*_{cond}(\rho,V,\Delta T)$. Let us especilally note that $T_Q\sim 10^2$ and $T_0\sim 10^3$ for metallic melts[22,43] so that ϵ can be small enough at a chosen value of j.

It is significant that the stitching functions formally satisfy the following asymptotic conditions $b_{cond}(\Delta T)\to 0$ if $\Delta T\to 0$ and $b_{conv}(\Delta T)\to 0$ if $\Delta T\to\infty$. Thus, $\sigma^*_{gen}\approx\sigma^*_{conv}$ at a small undercooling and $\sigma^*_{gen}\approx\sigma^*_{cond}$ at a large undercooling.

5 | UNDERCOOLING BALANCE

One or another selection criterion discussed in the previous section determines an equation, which connects the dendrite tip diameter ρ, tip velocity V, and undercooling ΔT. To find $\rho(\Delta T)$ and $V(\Delta T)$ we need a second law connecting ρ, V and ΔT. The undercooling balance represents such a condition.

Considering the case of convective boundary conditions (3) and (4) at the dendritic surface, we come to

$$\Delta T_{conv} = \Delta T_{Tconv} + \Delta T_{Cconv} + \Delta T_R + \Delta T_K. \tag{33}$$

Here the thermal ΔT_{Tconv} and concentration ΔT_{Cconv} contributions read as

$$\Delta T_{Tconv} = T_i - T_\infty = \frac{T_Q V k_s}{\alpha_h \rho_l c_l u_* D_T}, \quad \Delta T_{Cconv} = m(C_i - C_{l\infty}) = \frac{(1-k_0) V m C_{l\infty}}{\alpha_m u_* - (1-k_0)V}, \tag{34}$$

where the aforementioned analytical solutions (10) and (11) are taken into account.

The contributions ΔT_R and ΔT_K caused by the interface curvature (the Gibbs-Thomson effect) and the attachement kinetics of atoms at the dendritic interface can be written in the form of

$$\Delta T_R = \frac{4 d_0 T_Q}{\rho}, \quad \Delta T_K = \frac{V}{\mu_k}, \tag{35}$$

where μ_k is the kinetic coefficient. Note that expression (35) for ΔT_R is written in the three-dimensional case. In the case of two-dimensional grows this expression reads as $\Delta T_R = 2 d_0 T_Q / \rho$.[14]

Combining expressions (33)-(35), we obtain an explicit function

$$\rho(V, \Delta T_{conv}) = \frac{4 d_0 T_Q}{\Delta T_{conv} - \Delta T_{Tconv}(V) - \Delta T_{Cconv}(V) - V/\mu_k}. \tag{36}$$

In addition, the selection criterion (29) enables us to find the following implicit dependence defining the dendrite tip velocity V as a function of the melt undercooling ΔT_{conv}

$$\frac{\rho^2(V, \Delta T_{conv}) V \sigma^*_{conv}(\rho(V, \Delta T_{conv}), V)}{2 d_0 D_T} = 1. \tag{37}$$

Thus, equations (36) and (37) determine dependencies $\rho(\Delta T_{conv})$ and $V(\Delta T_{conv})$.

In the case of conductive mechanism of heat and mass transfer, the undercooling balance takes the form

$$\Delta T_{cond} = \Delta T_{Tcond} + \Delta T_{Ccond} + \Delta T_R + \Delta T_K, \tag{38}$$

where the thermal ΔT_{Tcond} and concentration ΔT_{Ccond} contributions are defined by expressions found in the previous studies.[6,14,15,22,24]

To obtain a generalized undercooling balance, we stitch together the convective and conductive balances (33) and (38) with the same stitching functions

$$\Delta T = \Delta T_{gen} = \frac{\Delta T_{conv} b_{conv}(\Delta T) + \Delta T_{cond} b_{cond}(\Delta T)}{b_{conv}(\Delta T) + b_{cond}(\Delta T)}. \tag{39}$$

Note that this condition has the same limiting properties as the selection criterion (31).

Thus, the generalized selection and balance laws (31) and (39) determine the dendrite tip diameter ρ and its velocity V as functions of the melt undercooling ΔT in the case of the mixed (convective and conductive) type of heat and mass transfer near the growing dendritic surface.

6 | DISCUSSION AND CONCLUSION

In this section, we analyze the behavior of analytical solutions for convective and conductive heat and mass transfer mechanisms and compare these cases. First of all, figure 2 demonstrates the dendrite tip velocity versus the melt undercooling calculated for both conductive (expressions (30) and (38)) and convective (expressions (36) and (37)) heat and mass transfer mechanisms. So, for example, if we use the classical (conductive) boundary conditions, none of the blue dashed and green dash-dotted lines can describe experimental data for small undercooling. What is more, increasing the rate U of incoming forced flow, the "conductive" curve shifts to the right (to greater undercooling) and moves away from experimental data. In other words, by

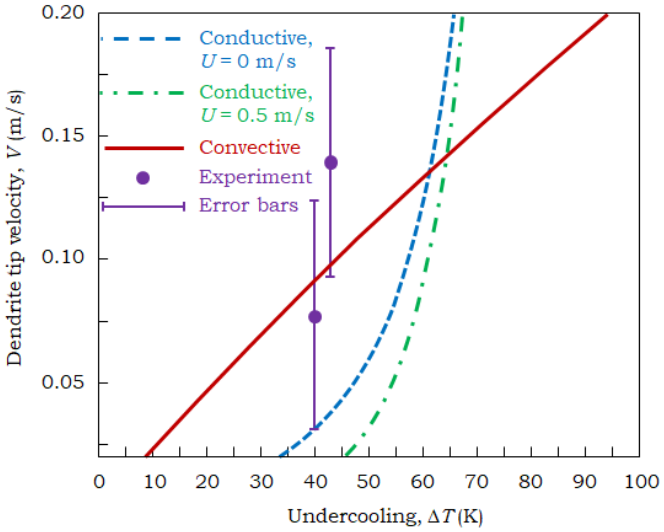

FIGURE 2 Dendrite tip velocity V as a function of the melt undercooling ΔT for $Ti_{45}Al_{55}$ melt. The dashed (blue) and dash-dotted (green) curves are plotted for the conductive heat and mass transfer mechanism without ($U = 0$ m/s) and with ($U = 0.5$ m/s) the forced fluid flow (expressions (30) and (38)). The solid line (red) is illustrated accordingly to expressions (36) and (37). Theoretical predictions are compared with experimental data[44] for small undercoolings. The model parameters are $\sigma_0 = 1.17$, $n = 4$, $d_0 = 9.28 \cdot 10^{-10}$ m, $D_T = 2.5 \cdot 10^{-6}$ m^2 s^{-1}, $\rho_l = 2.46 \cdot 10^3$ kg m^{-3}, $k_0 = 0.86$, $C_{l\infty} = 55$ at%, $\alpha_d = 0.3$, $\beta_0 = 1.88 \cdot 10^{-2}$ s m^{-1}, $\mu_k = 10^{-3}$ m s^{-1} K^{-1}, $m = 8.78$ K at%$^{-1}$, $c_l = 1237$ J kg^{-1} K^{-1}, $\alpha_h = 3.55$, $\alpha_m = 1$, $u_* = 4$ m s^{-1}, $T_Q = 272.64$ K, $k_s = 29.22$ W m^{-1} K^{-1}, $A_n = A_4 = 1$.

changing the parameter U it is not possible to combine the "conductive" theory with measurements. However, if we use the "convective" theory under consideration, it is possible to describe experiments. Indeed, the red solid line is within the error bars of measurements.

From the physical point of view, this behavior is explained by the fact that the intense fluid flow can arise near the growing crystals. In turn, this flow is responsible for a transition from the laminar regime to the turbulent one in levitated droplets.[45] Such a transition can be caused by the presence of intense fluid curls leading to the convective heat and mass transfer mechanism near dendritic tips (where the flow can be turbulent[45]). Therefore, given all the above, we conclude that the "convective" boundary conditions leading to the model expressions (36) and (37) of stable dendritic growth, where σ^*_{conv} is defined by the selection criterion (29), can describe experimental data for small undercooling.

Figure 3 illustrates the wider diapason of undercooling from the same experimental work. As would be expected, the convective model (36) and (37) well describes experiments in the range of small undercooling (blue line in figure 3). However, the range of large undercooling is described well by the conductive model (30) and (38). Describing the intermediate region in ΔT as well as the whole undercooling diapason, we must use the generalized stitched model (31) and (39), which well describes experimental data in figure 3 . In other words, describing all undercooling range in the case of intense convection near the growing dendrites, one can use the mixed (conductive and convective) heat and mass transfer mechanism corresponding to the generalized stitched model (31) and (39), where the stitching functions are given by expressions (32). As this takes place, their parameters i_{conv}, i_{cond}, j_{conv} and j_{cond} should be chosen in such a manner to achieve a better fitting between the theory and experimental data. Let us especially note in conclusion that the stitching functions can be chosen in diverse ways with the limit transitions to the "convective" and "conductive" models. This question represents an interesting and important topic for future research.

As a special note, the present theory of stable dendritic growth with convective heat and mass transfer can be extended in describing such phenomena as dendritic growth at the inner core boundary of the Earth,[46] the evolution of crystals in magma chambers and lava lakes,[47] as well as in mushy layers of sea ices[48–50] or, in other words, wherever convective heat and mass transfer plays an important role.

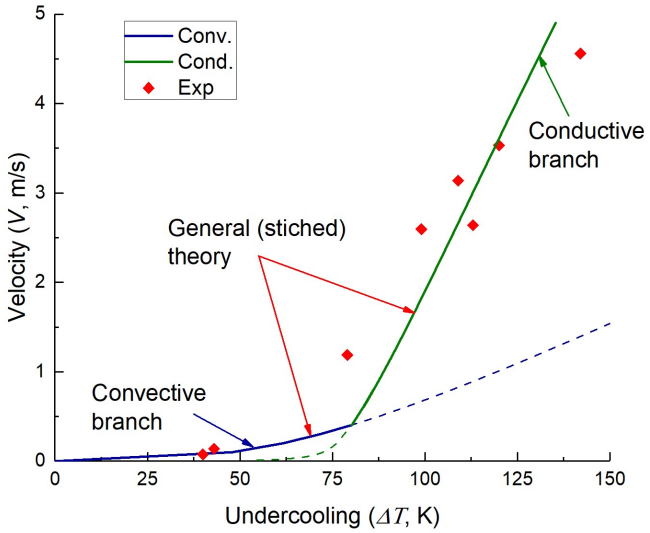

FIGURE 3 Dendrite tip velocity V as a function of the melt undercooling ΔT for $Ti_{45}Al_{55}$ melt (experimental points are taken from Hartmann et al.[44]). Two experimental points lying near 40 K are the same as the points shown in figure 2 . The model parameters correspond to figure 2 and $D_C = 8.27 \cdot 10^{-9}$ m^2 s^{-1}, $T_0 = 1748$ K, $\epsilon_{conv} = 3 \cdot 10^{-9}$, $\epsilon_{cond} = 0.03$, $j_{conv} = j_{cond} = 3$, $\tilde{b} = 0.1$.

ACKNOWLEDGMENTS

The present work comprises different parts of research studies including (i) the model formulation, stability and solvability analyses, derivation of the selection criterion in the case of intense convection, its sewing with the criterion for the conductive boundary conditions, (ii) numerical simulations, (iii) experiments, and their comparison. Different parts of the present work were supported by different grants and programs. With this in mind, the authors are grateful to the following foundations, programs, and grants.

Theoretical part (i) was supported by the Russian Foundation for Basic Research (grant no. 19-32-51009). Numerical part (ii) was made possible due to the financial support of the Ministry of Science and Higher Education of the Russian Federation (Ural Mathematical Center, project no. 075-02-2020-1537/1). The experimental part (iii) was supported by the German Space Center Space Management under contract number 50WM1941.

Author contributions

The authors contributed equally to the present research article.

Conflict of interest

The authors declare no potential conflict of interests.

ORCID

Liubov V. Toropova https://orcid.org/0000-0003-4587-2630
Dmitri V. Alexandrov https://orcid.org/0000-0002-6628-745X
Peter K. Galenko https://orcid.org/0000-0003-2941-7742

References

1. Trivedi R, Kurz W. Dendritic growth. *Int. Mater. Rev.*. 1994;39:49–74.
2. Kurz W, Fisher DJ. *Fundamentals of Solidification*. Aedermannsdorf: Trans. Tech. Publ.; 1989.
3. Herlach D, Galenko P, Holland-Moritz D. *Metastable Solids from Undercooled Melts*. Amsterdam: Elsevier; 2007.
4. Pelcé P.. *Dynamics of Curved Fronts*. Boston: Academic Press; 1987.
5. Galenko PK, Alexandrov DV. From atomistic interfaces to dendritic patterns. *Phil. Trans. R. Soc. A*. 2018;376:20170210.
6. Alexandrov DV, Galenko PK, Toropova LV. Thermo-solutal and kinetic modes of stable dendritic growth with different symmetries of crystalline anisotropy in the presence of convection. *Phil. Trans. R. Soc. A*. 2018;376:20170215.
7. Libbrecht K.. *Snowflakes*. Minneapolis, MN: Voyageur Press; 2004.
8. Kessler DA, Koplik J, Levine H. Pattern selection in fingered growth phenomena. *Adv. Phys.*. 1988;37:255–339.
9. Alexandrov DV, Zubarev AYu. Patterns in soft and biological matters. *Phil. Trans. R. Soc. A*. 2020;378:20200002.
10. Gusakova OV, Galenko PK, Shepelevich VG, Alexandrov DV, Rettenmayr M. Diffusionless (chemically partitionless) crystallization and subsequent decomposition of supersaturated solid solutions in Sn-Bi eutectic alloy. *Phil. Trans. R. Soc. A*. 2019;377:20180204.
11. Brener EA, Temkin DE. Dendritic growth at deep undercooling and transition to planar front. *Europhys. Lett.*. 1989;10:171–175.
12. Alexandrov DV, Galenko PK. The shape of dendritic tips. *Phil. Trans. R. Soc. A*. 2020;378:20190243.
13. Brener EA, Mel'nikov VI. Pattern selection in two-dimensional dendritic growth. *Adv. Phys.*. 1991;40:53–97.
14. Alexandrov DV, Galenko PK. Dendritic growth with the six-fold symmetry: theoretical predictions and experimental verification. *J. Phys. Chem. Solids*. 2017;108:98–103.
15. Alexandrov DV, Galenko PK. Thermo-solutal growth of an anisotropic dendrite with six-fold symmetry. *J. Phys.: Condens. Matter*. 2018;30:105702.
16. Ivantsov GP. Temperature field around spherical, cylinder and needle-like dendrite growing in supercooled melt. *Dokl. Akad. Nauk SSSR*. 1947;58:567–569.
17. Ivantsov GP. On a growth of spherical and needle-like crystals of a binary alloy. *Dokl. Akad. Nauk SSSR*. 1952;83:573–575.
18. Horvay G, Cahn JW. Dendritic and spheroidal growth. *Acta Metall.*. 1961;9:695–705.
19. Galenko PK, Alexandrov DV, Titova EA. The boundary integral theory for slow and rapid curved solid/liquid interfaces propagating into binary systems. *Phil. Trans. R. Soc. A*. 2018;376:20170218.
20. Ben Amar M, Pelcé P. Impurity effect on dendritic growth. *Phys. Rev. A*. 1989;39:4263–4269.
21. Bouissou Ph, Pelcé P. Effect of a forced flow on dendritic growth. *Phys. Rev. A*. 1989;40:6673–6680.
22. Alexandrov DV, Galenko PK. Dendrite growth under forced convection: analysis methods and experimental tests. *Phys.-Usp.*. 2014;57:771–786.
23. Alexandrov DV, Galenko PK, Herlach DM. Selection criterion for the growing dendritic tip in a non-isothermal binary system under forced convective flow. *J. Cryst. Growth*. 2010;312:2122–2127.
24. Alexandrov DV, Galenko PK. Thermo-solutsl and kinetic regimes of an anisotropic dendrite growing under forced convective flow. *Phys. Chem. Chem. Phys.*. 2015;17:19149–19161.

25. Alexandrov DV, Galenko PK. Selection criterion of stable mode of dendritic growth with n-fold symmetry at arbitrary Péclet numbers with a forced convection. In: Gutschmidt S, Hewett JN, Sellier M, eds. *IUTAM Symposium on Recent Advances in Moving Boundary Problems in Mechanics*, IUTAM Bookseries 34. Springer 2019 (pp. 203–215).

26. Alexandrov DV, Galenko PK. Selected mode for rapidly growing needle-like dendrite controlled by heat and mass transport. *Acta Mater.*. 2017;137:64–70.

27. Alexandrov DV, Danilov DA, Galenko PK. Selection criterion of a stable dendrite growth in rapid solidification. *Int. J. Heat Mass Trans.*. 2016;101:789–799.

28. Galenko PK, Danilov DA, Reuther K, Alexandrov DV, Rettenmayr M, Herlach DM. Effect of convective flow on stable dendritic growth in rapid solidification of a binary alloy. *J. Cryst. Growth.* 2017;457:349–355.

29. Notz D, McPhee MG, Worster MG, Maykut GA, Schlünzen KH, Eicken H. Impact of underwater-ice evolution on Arctic summer sea ice. *J. Geophys. Res.*. 2003;108:3223.

30. Alexandrov DV, Nizovtseva IG. To the theory of underwater ice evolution, or nonlinear dynamics of 'false bottoms'. *Int. J. Heat Mass Trans.*. 2008;51:5204–5208.

31. Pelcé P, Bensimon D. Theory of dendrite dynamics. *Nucl. Phys. B.* 1987;2:259–270.

32. McPhee MG, Maykut GA, Morison GH. Dynamics and thermodynamics of the ice/upper ocean system in the marginal ice zone of the Greenland Sea. *J Geophys Res.* 1987;92:7017–7031.

33. Alexandrov DV, Malygin AP. Convective instability of directional crystallization in a forced flow: the role of brine channels in a mushy layer on nonlinear dynamics of binary systems. *Int. J. Heat Mass Trans.*. 2011;54(1):1144–1149.

34. Alexandrov DV, Bashkirtseva IA, Ryashko LB. Nonlinear dynamics of mushy layers induced by external stochastic fluctuations. *Phil. Trans. R. Soc. A*. 2018;376:20170216.

35. Tritton DJ. *Physical Fluid Dynamics*. Oxford, UK: Clarendon Press; 1988.

36. Owen PR, Thomson WR. Heat transfer across rough surfaces. *J. Fluid Mech.*. 1963;15:321–334.

37. Yaglom AM, Kader BA. Heat and mass transfer between a rough wall and turbulent flow at high Reynolds and Peclet numbers. *J. Fluid Mech.*. 1974;62:601–623.

38. Alexandrov DV, Nizovtseva IG, Lee D, Huang H-N. Solidification from a cooled boundary with a mushy layer under conditions of nonturbulent and turbulent heat and mass transfer in the ocean. *Int. J. Fluid Mech. Res.*. 2010;37:1–14.

39. Barbieri A, Langer JS. Predictions of dendritic growth rates in the linearized solvability theory. *Phys. Rev. A*. 1989;39:5314–5325.

40. Toropova LV, Alexandrov DV, Rettenmayr M, Galenko PK. The role of intense convective flow on dendrites evolving with n-fold symmetry. *J. Cryst. Growth.* 2020;535:125540.

41. Toropova LV, Galenko PK, Alexandrov DV, Demange G, Kao A, Rettenmayr M. Theoretical modeling of crystalline symmetry order with dendritic morphology. *Eur. Phys. J. Special Topics.* 2020;229(2–3):275–286.

42. Kao A, Toropova LV, Alexandrov DV, Demange G, Galenko PK. Modeling of dendrite growth from undercooled nickel melt: Sharp interface model versus enthalpy method. *J. Phys.: Condens. Matter.* 2020;32(19):194002.

43. Galenko PK, Reuther K, Kazak OV, Alexandrov DV, Rettenmayr M. Effect of convective transport on dendritic crystal growth from pure and alloy melts. *Appl. Phys. Lett.*. 2017;111:031602.

44. Hartmann H, Galenko PK, Holland-Moritz D, Kolbe M, Herlach DM, Shuleshova O. Non-equilibrium solidification in undercooled $Ti_{45}Al_{55}$ melts. *J. Appl. Phys.*. 2008;103:073509.

45. Hyers RW, Trapaga G, Abedian B. Laminar-turbulent transition in an electromagnetically levitated droplet. *Metall. Mater. Trans. B.* 2003;34B:29–36.

46. Alexandrov DV, Galenko PK. Selection criterion for the growing dendritic tip at the inner core boundary. *J. Phys. A: Math. Theor.*. 2013;46:195101.

47. Alexandrov DV, Netreba AV, Malygin AP. Time-dependent crystallization in magma chambers and lava lakes cooled from above: The role of convection and kinetics on nonlinear dynamics of binary systems. *Int. J. Heat Mass Trans.*. 2012;55:1189–1196.

48. Alexandrov DV, Bashkirtseva IA, Malygin AP, Ryashko LB. Sea ice dynamics induced by external stochastic fluctuations. *Pure Appl. Geophys.*. 2013;170:2273–2282.

49. Nizovtseva IG, Alexandrov DV. The effect of density changes on crystallization with a mushy layer. *Phil. Trans. R. Soc. A*. 2020;378:20190248.

50. Alexandrova IV, Alexandrov DV. Dynamics of particulate assemblages in metastable liquids: A test of theory with nucleation and growth kinetics. *Phil. Trans. R. Soc. A*. 2020;378:20190245.

How to cite this article: Toropova L.V., and Alexandrov D.V., and Galenko P.K. (2020), Selection criteria for the n-fold symmetry of dendritic growth in the presence of convective flow, *Math Meth Appl Sci.*,